Biosensors and Bioelectronics 68 (2015) 181–188

Contents lists available at ScienceDirect

Biosensors and Bioelectronics

journal homepage: www.elsevier.com/locate/bios

Poly (9-(2-diallylaminoethyl)adenine HCl-co-sulfur dioxide) deposited on silica nanoparticles constructs hierarchically ordered nanocapsules: Curcumin conjugated nanocapsules as a novel strategy to amplify guanine selectivity among nucleobases

Mai Mouslmani, Kamal H. Bouhadir, Digambara Patra *

Department of Chemistry, American University of Beirut, Beirut, Lebanon

ARTICLE INFO

Article history:
Received 13 October 2014
Received in revised form
11 December 2014
Accepted 15 December 2014
Available online 17 December 2014

Keywords:
Poly A
Curcumin
Silica NPs
Guanine
Nucleobases
Selectivity

ABSTRACT

Poly (9-(2-diallylaminoethyl)adenine HCl-co-sulfur dioxide) (Poly A) deposited on silica nanoparticles self-assembles to form hierarchically ordered nanocapsules. These nanocapsules can be conjugated with curcumin. The curcumin-conjugated nanocapsules are found to be spherical in size and their size ranges between 200 and 600 nm. We found that curcumin conjugated with silica nanoparticles marginally shows a selectivity (~20%) for guanine over adenine, cytosine, thymine and uracil, but this selectivity is extraordinarily amplified to more than 500% in curcumin-conjugated nanocapsules prepared from the above procedure. FT-IR spectra along with lifetime measurements suggest that specific interaction between adenine moieties of Poly A nanocapsules and thymine/uracil does not affect the fluorescence of poly A nanocapsules. Thus, the sensitivity and selectivity for guanine estimation is due to hydrophobic interactions, which are assisted by the low water solubility of guanine as compared to the other nucleobases. The present method illustrates a wider linear dynamic range in the higher concentration range as compared to the reported methods. Finally, the degradation study proves that stability of curcumin is improved dramatically in such nanocapsules demonstrating that nanotechnology could be a viable method to improve selectivity of specific analyte and robustness of probe molecule during fluorescence based bio-sensing.

1. Introduction

Nanotechnologies and nanomaterials are getting widely utilized in sensor designing since past 10 years (Zhang et al., 2009). During this period this field has witnessed fast development and advancement. The importance of nanomaterials is not only referred to their geometric size but also due to the fact that a change from macro-/micro- to nano-scale qualitatively changes the physicochemical characteristics such as magnetism, optical refraction, electric conductivity, thermal stability and strength, light absorption and emission. It also produces new materials of the same chemical nature, but having properties and reactivity that are lacking in macro- and micro-scopic materials, thus opening new possibilities for sensor designing. All types of nanoparticles can be incorporated into different inorganic and organic materials to develop nanoscale sensors. Such nanosensors can be applied in both gas and liquid media analysis (Shtykov and Rusanova, 2008). Recently, there have been tremendous demands for utilizing nanomaterials as biosensing probes. Based on the hybridization between a target and its complementary probe, various electrochemical and optical methods have been successfully used (Sassolas et al., 2008).

The introduction of nucleic acids' fluorescent labeling method has opened up the ability of utilizing such systems for further research and development. The recent years have witnessed rapid growth of fluorescent probes as well as wide development of homogenous fluorescence assays, including those based on fluorescence resonance energy transfer (FRET) or quenching mechanisms for nucleic acid detection (Didenko, 2006). These probes like molecular beacons are labeled with both a quencher dye and a fluorescent reporter, where the reporter fluoresces when the two dyes are physically separated after the hybridization (Wang et al., 2011). At the same time determination and separation of nucleobases is an important and challenging task due to the significance of these compounds in numerous biological processes. Adenine (A), cytosine (C), guanine (G), thymine (T) and uracil (U) are the building blocks of both RNA and DNA that play an important role in the storage of genetic information and protein biosynthesis

* Corresponding author. Fax: +961 1365217.
E-mail address: dp03@aub.edu.lb (D. Patra).

http://dx.doi.org/10.1016/j.bios.2014.12.036
0956-5663/

(Brown, 1987). Thus, the identification and estimation of individual nucleobases are crucial to understand the sequence of nucleic acids (Blazej et al., 2005). DNA sequencing has been of great interest for human genomics, forensic sciences, genetic engineering and medicinal applications. Selective estimation of individual nucleobases has tremendous potential application during DNA sequencing (Adams et al., 2007). Besides being one of the building blocks of DNA/RNA (to store genetic information and for protein biosynthesis) (Wang et al., 2008), guanine concentration is used to measure degree of oxidative damage to DNA (Li et al., 2012), because guanine is easily oxidized by different types of oxidants and free radicals (Li et al., 2012; Abbaspour and Noori, 2008). The widespread effect of guanine on cerebral circulation and coronary, control of blood flow, prevention of cardiac arrhythmias, modulation of adenylate cyclase activity, inhibition of neutrotransmitter release, etc. Zhu et al. (2013) have made guanine estimation a challenging and crucial task in clinical medicine, biological science and analytical chemistry.

Available methods for guanine estimation based on electrochemical assays, chromatography and capillary electrophoresis suffer due to labor-intensive electrode procedures, poor stability of electrodes or complicated and expensive equipment. The simple, fast and selective fluorescence method has attracted for selective determination of nucleobase. Further fluorescence markers are widely used in electrophoresis where a fluorescent marker specific to particular nucleobase may ease the analytical procedure during nucleic acid sequencing (Mahmodian et al., 2008). The interaction of gold nanoparticles and nucleobases has been reported, where experiments showed that A, G, C and T specifically interact in a sequence based manner with the surfaces of gold (Sharma et al., 2007). Moreover, the interaction of organic nanoparticles with nucleobases has been investigated showing different fluorescence responses for the four nucleobases (Xu et al., 2008).

In the present work, we have applied the method of self assembly to synthesize nanocapaulses based on Poly (9-(2-diallylaminoethyl)adenine HCl-co-sulfur dioxide) (Poly A). Poly A as prepared in our lab is a polymer of adenine along with a poly amine backbone. In this nanocapsule formation method, Poly A is deposited on silica nanoparticles (NPs) to which curcumin is incorporated subsequently as a fluorescence probe for the detection of nucleobases, in specific for the estimation of guanine. The nanocapsules are of various sizes ranging from 200 to 600 nm. The detection mode is based on the change in the fluorescence intensity of curcumin. The advantages of such technique are: (i) synthetic procedure is easy, (ii) it does not require long hours of nanocapsules preparation, (iii) materials are stable and robust, (iv) it is highly selective for guanine among nucleobases and, (v) it has a wider linear dynamic range.

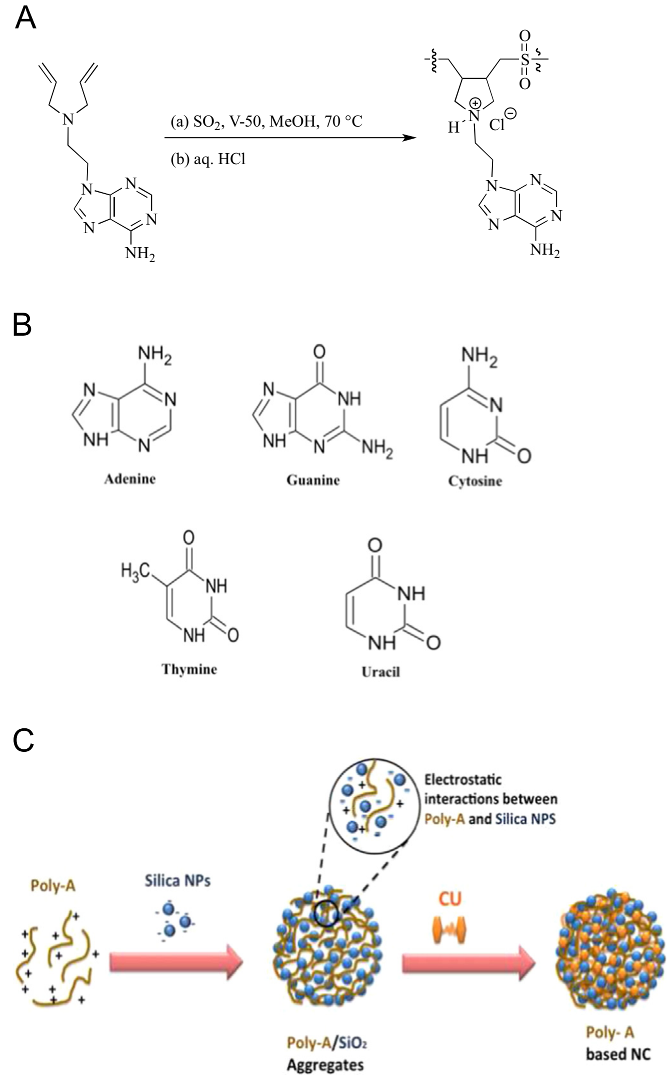

Fig. 1. (A) Chemical structure of Poly (9-(2-diallylaminoethyl)adenine HCl-co-sulfur dioxide) (Poly A). (B) The nucleobases used and their corresponding chemical structure. (C) Illustration of Poly A interacting with SiO_2 NPs, and curcumin to form nanocapsules.

2. Materials and methods

2.1. Materials

Curcumin was obtained from Acros Organics. Poly A was synthesized as shown in Fig. 1A using a procedure explained earlier (Bouhadir et al., 2012). The nucleobases including adenine, guanine, cytosine, thymine and uracil (structure shown in Fig. 1B) were obtained from Sigma-Aldrich and their stock solutions were prepared in de-ionized water. Silica LUDOX® HS-40 Colloidal Silica was also obtained from Sigma-Aldrich.

2.2. Preparation of Poly A nanocapsule

Encapsulation of curcumin inside the nanocapsules was made using Poly A as the structure directing agent. In this process 1.3 mL of Poly A (2 mg mL^{-1}) was gently vortex mixed for 20 s with 7.8 mL of negatively charged silica nanoparticles. The obtained cloudy suspension was aged for 2 h; then it was centrifuged for 20 min at a speed of 4450 rpm. Poly A and SiO_2 aggregates were collected. To the latter precipitate 0.5 ml of curcumin (1 mg mL^{-1} prepared in 10% acetone/de-ionized water solution) and 2.5 ml of de-ionized water were added. The mixture was allowed to age for 30 min, and again centrifuged for 20 min at a speed of 4450 rpm. The precipitate of nanocapsules formed was washed with de-ionized water for 3 times to remove the excess of curcumin. The preparation method is depicted in Fig. 1C. Finally it was dispersed in 3 mL of de-ionized water for further characterization and investigation.

2.3. Morphological characterization

Scanning electron microscopy (SEM) analysis was done using a Tescan, Vega 3 LMU with Oxford Edx detector (Inca XmaW20) SEM, where 3 mg of the nanocapules was dissolved in 5 ml of de-ionized water, and a few drops of the nanocapsule suspension were mounted on an aluminum stub, coated with carbon adhesive. After being dried the sample was ready for the SEM analyses. The particle size distribution was analyzed using a DLS (Brookhaven Instruments Corps) technique with a laser source of 658 nm and a PMT detector (HAMAMATSU, HC120-30). The software used was 90Plus Particle Sizing Software Ver. 5.23 and the dust was set at 40.

2.4. Spectroscopic measurements

FT-IR spectra were recorded using a Thermo Scientific Nicolet iS5 FT-IR Spectrophotometer where the sample was placed on the crystal plate and sealed with the tip. The absorption spectra were recorded using a JASCOV-570 UV–vis–NIR Spectrophotometer at room temperature. The steady-state fluorescence spectra (excitation and emission) were recorded at room temperature using Jobin-Yvon-Horiba Fluorolog III fluorometer and the FluorEssence program where the excitation and emission slits width was 5 nm. The source of excitation was a 100 W Xenon lamp, and the detector used was R-928 operating at a voltage of 950 V. The fluorescence lifetime measurements were done using the same instrument except a pulsed diode laser of excitation wavelength 405 nm was used for excitation. Instrumental response (prompt) for lifetime measurement was carried out using colloidal non-fluorescent particles. The decay data were analyzed using Data Analysis Software.

3. Results and discussion

When curcumin was mixed with silica nanoparticles, the fluorescence emission spectrum showed a large blue-shift from ~550 nm in water to around 495 nm. This large shift might not be due to change in local environment (Patra and Barakat, 2011), unlike the case observed for curcumin embedded in the phospholipid membranes (Patra et al., 2012). The bulk solvent environment of silica particles is still an aqueous medium; therefore, such shift could only be explained based on the strong association of curcumin with silica particles. Interaction of curcumin–silica NPs complex with different nucleobases (see Fig. 2A) very slightly shifted the maximum towards the lower wavelength range. However, when the fluorescence intensity of curcumin–silica NPs complex was compared in the presence of different bases (fixing the concentration at 1 mg/mL for nucleobases), the fluctuation of fluorescence intensity, which was measured at around emission maximum, illustrated a different behavior. Fig. 2B depicts that the fluorescence intensity of curcumin–silica NPs complex was marginally quenched in the presence of most of the nucleobases (3% for uracil, 5% for thymine, 9% for adenine and 15% for cytosine) except for guanine, in which case a remarkable 20% enhancement of fluorescence intensity was observed. Although this trend is positive, the change is not significant to get a conclusive selectivity for guanine for fluorescence sensing in the presence of other nucleobases.

To further improve the effectiveness towards selective sensing for guanine, we tested a synthesized polymer, Poly A, which contains adenine moieties along with polyamine backbone. The structure is shown in Fig. 1A. In this case silica nanoparticles were mixed with Poly A and then curcumin was added to form large aggregates as explained in Section 2. The pre-synthesized data, controlled experimental conditions and optimized data for synthesis of such aggregated complex (or nanocapsules) using

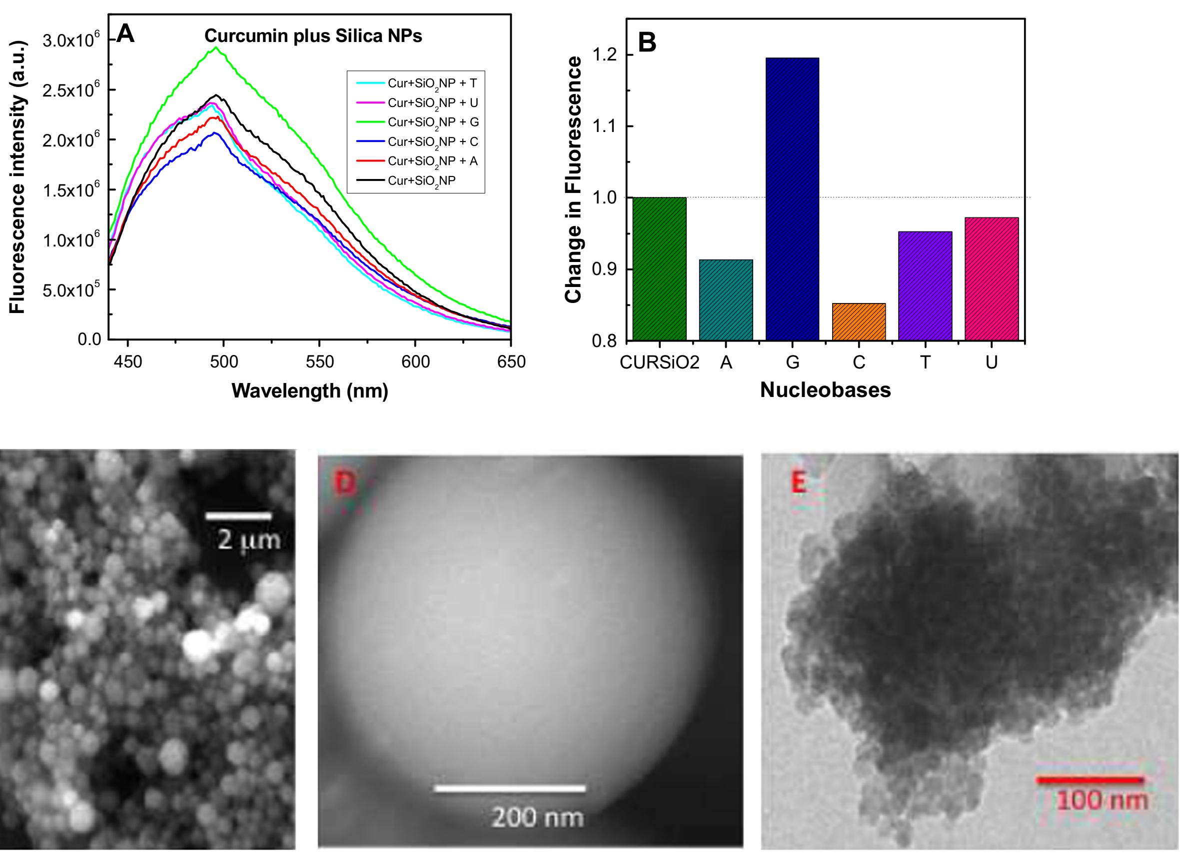

Fig. 2. (A) Fluorescence spectra of curcumin with silica NPs in the presence of various nucleobases excited at 425 nm, where the concentrations of curcumin and nucleobases were fixed at 5 μM and 1 mg/ml, respectively. (B) Relative change in fluorescence intensity of curcumin with silica NPs in the presence of nucleobases when the fluorescence intensity of curcumin with silica NPs without nucleobase was normalized to 1. The excitation wavelength was 425 nm and the emission wavelength was 495 nm. (C) SEM images of nanocapsules containing silica NPs, curcumin and Poly adenine (Poly A) at 500 nm resolution and (D) 200 nm resolution. (E) TEM image of silica NPs used at 100 nm resolution.

negatively charged particles/ions and positively charged polymer are reported by us elsewhere (Mauslmani and Patra, 2014); therefore, we did not repeat to investigate mechanism of nanocapsules formation in the present case. At the same time, these aggregates were characterized using SEM and DLS method. The particle size distribution was analyzed by a dynamic light scattering (DLS) technique and was found to have an effective hydrodynamic radius (R_h) of 700 nm. However, the SEM images of Poly A aggregates (Fig. 2C and D) showed that the aggregates were found to be of various sizes from 200 to 600 nm, and most of them were less than 500 nm. This high effective diameter is due to the further aggregation of smaller size aggregates in solution. These aggregates were found to be spherical. This can be explained by the fact that negative charge of silica nanoparticles (see Fig. 2E) encouraging Poly A, having positive charge, to get adsorbed on its surfaces, which further facilitates the self-assembly of Poly A into spherical nanocapsules. We have found earlier similar observations for negatively charged salt and polyamine systems (Mauslmani and Patra, 2014; Patra et al., 2009). In the present case curcumin does not play a major role during the nanocapsules' formation which is evident from the fact that when Poly A was mixed with curcumin and then silica nanoparticles were added to the latter mixture, no nanocapsules were observed. At the same time concentration of silica nanoparticles was important to determine the size of the nanocapsules (Mauslmani and Patra, 2014). We also decided to choose nanocapsules of this size ranges due to better yield of nanocapsule. It should be noted that during the preparation of Poly A nanocapsules, the unreacted polymer, silica and curcumin were washed out by centrifugation after the formation of the nanocapsules as explained in Section 2. The self-assembly of poly A polymer was further established from the change in FT-IR spectrum. The FT-IR spectra of Poly A polymer and Poly A based nanocapsules depicted in Fig. 3A indicate a remarkable difference between the FT-IR spectra of the two cases. The prominent peak at around 3422 cm^{-1} of Poly A polymer was not detected for the Poly A based nanocapsules. This peak could be due to amino group present in Poly A, and its absence in the nanocapsule could be explained by the expected strong interaction between silica particles and positive charge of amino group. The thermogravimetric analysis (TGA) was used to quantify silica, Poly A and curcumin content in the nanocapsules. TGA data of raw curcumin indicated that the weight-loss occurs around 260 °C and continues till 550 °C. Poly A also gave a similar weight loss (Bouhadir et al., 2012). The degradation of Poly A at lower temperature has been related to breakdown of the thermally sensitive adenine moiety (Bouhadir et al., 2012). Unfortunately, over all thermal degradation of both Poly A and curcumin was found to be located in the same temperature region. Thus, to quantify curcumin content in the nanocapsules, spectrophotometric measurements were done for curcumin before addition to the reaction medium and curcumin washed out in each step. It was found that about 4% of curcumin was present in the nanocapsules, whereas 6% of nanocapsules was Poly A as obtained from TGA data after subtracting curcumin content. The TGA data also confirmed substantial part, ~90%, of the materials in the nanocapsules as silica.

The fluorescence emission spectrum of Poly A based nanocapsules (see Fig. 3B) was centered at ~548 nm. This emission maximum is a remarkable red-shift from 495 nm found earlier for curcumin in the presence of silica nanoparticles; however it is similar to one found for curcumin in poly (allyl amine

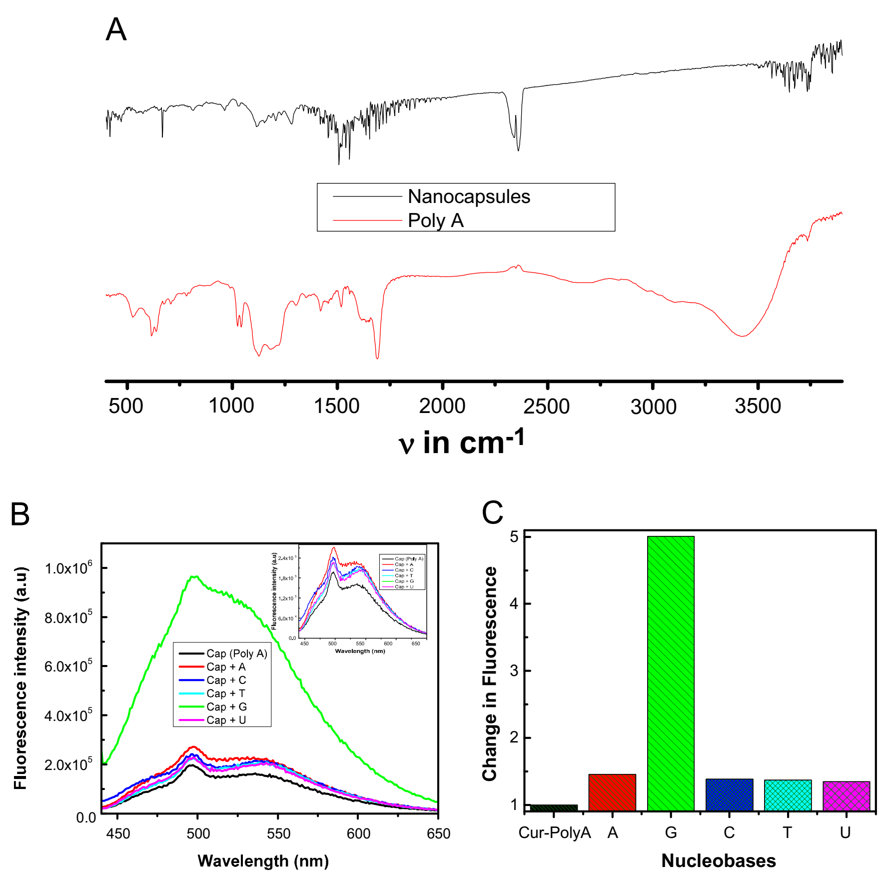

Fig. 3. (A) The FT-IR spectra of Poly A polymer and Poly A based nanocapsules. (B) Fluorescence spectra of nanocapsules containing silica NPs, Poly A and curcumin in the presence of various nucleobases excited at 425 nm. The concentration of the capsule and nucleobases was fixed at 1 mg/ml (inset shows rescaled spectra of nanocapsules without guanine). (C) Relative change in fluorescence intensity of Poly A nanocapsules in the presence of nucleobases when the fluorescence intensity of Poly A nanocapsules without nucleobase was normalized to 1. The excitation wavelength was 425 nm and the emission wavelength was 543 nm.

hydrochloride) (PAH) based nanocapsules (Mauslmani and Patra, 2014). This signifies that curcumin is directly linked with Poly A rather than silica nanoparticles during the nanocapsules formation. Note that in case of PAH (Mauslmani and Patra, 2014), PAH nanocapsules were prepared using salt (dipotassium hydrogen phosphate) over which silica and curcumin were deposited, whereas in the present case it is rather a deposition of poly A on the surface of silica nanoparticles. Thus, the slight variation of spectral shift in these two different preparation modes is due to the variation in the local environment of curcumin. Such local environment is expected where silica nanoparticles were put over PAH and curcumin in the case of PAH nanocapsules (Mauslmani and Patra, 2014). On the contrary, in the present case silica NPs and poly A initially form a complex over which curcumin was deposited. Thus, a strong silica–curcumin association is expected in the case of PAH nanocapsules (Mauslmani and Patra, 2014) but a strong interaction between curcumin and Poly A is expected in the present case. Notably, the fluorescence intensity of curcumin decreased substantially in Poly A based nanocapsules (containing poly A, silica nanoparticles and curcumin) compared to that of curcumin–silica NPs complex. This decrease in fluorescence intensity in Poly A based nanocapsules can be explained based on the fact that during self-assembly process of nanocapsule formation curcumin molecules present within the nanocapsule are forced to come close together, which encourages homo energy transfer (self-quenching) among curcumin molecules, thus, reduces the fluorescence intensity. At the same time individual curcumin–silica NPs are expected to be far from each other in solution, which reduces possibility of self-quenching among curcumin molecules.

Interestingly, addition of nucleobases did not change the emission maximum of these nanocapsules appreciably except for guanine. Herein, when guanine was added a further blue-shift of 10 nm was observed, indicating a remarkable interaction between guanine and curcumin conjugated Poly A based nanocapsules. Nevertheless, the change in selectivity towards guanine for fluorescence assessment was highly remarkable. The fluorescence intensity increase (measured at around emission maximum) in the presence of most of the other nucleobases was nominal, in the range 20–40%, while in the presence of guanine the fluorescence enhancement was 500% (see Fig. 3C).

The fluorescence lifetime decay profile at $\lambda_{ex}=$ 405 nm and $\lambda_{em}=$ 540 nm for poly A based nanocapsule in the absence and presence of nucleobases in water could be best fitted with a biexponential decay giving a short component lifetime (τ_1) of ~533 ps (83%) and long component lifetime (τ_2) of 4.33 ns (17%). However, in ultrafast femtosecond time-resolved measurement other smaller lifetime components for curcumin have been reported (Adhikari et al., 2009; Adhikary et al., 2010), which were not resolved in our present instrumental conditions. Nevertheless, the biexponential decay and such values are not surprising because similar lifetime values of this time scale in different solvents for curcumin have been reported in literature (Khopde et al., 2000). The fluorescence lifetime values of Poly A based nanocapsules marginally increased in the presence of cytosine [τ_1=558 ps (84%) and τ_2=4.48 ns (16%)], thymine [τ_1=569 ps (85%) and τ_2=4.22 ns (15%)], and adenine [τ_1=598 ps (77%) and τ_2=4.79 ns (23%)]. A decrease was observed for uracil [τ_1=480 ps (80%) and τ_2=3.5 ns (20%)]. Though, the value for long component was found to be 4.73 ns (19%) in the presence of guanine, the short component species increased appreciably in the presence of guanine. These variations of fluorescence lifetime of poly A based nanocapsules in the presence of nucleobases could be explained considering two cases: (i) interaction of the nanocapsules with the nucleobases due to hydrophobic and other electrostatic interactions and, (ii) association of the nanocapsules with the nucleobases because of specific base pairings. The improvement in short component as well as long component lifetime of the Poly A based nanocapsules in the presence of adenine, cytosine, and guanine could be due to hydrophobic interaction between the nucleobase and Poly A nanocapsules, whereas the decrease in long component lifetime in the presence of thymine and uracil is caused by specific base pair interaction between adenine moiety present in Poly A nanocapsule and thymine/uracil. The decrease in short component lifetime in the presence of uracil could also be referred to the same reason whereas the increase in short component lifetime of Poly A nanocapsules in the presence of thymine does not rule out hydrophobic interaction along with specific base pair interaction between thymine and Poly A nanocapsule.

To establish the above stated facts, we measured the FT-IR spectrum of different nucleobases and compared them with that of mixture of poly A based nanocapsules and nucleobases. There was no remarkable difference between the FT-IR spectra of individual adenine or cytosine compared to those of Poly A based nanocapsules in the presence of adenine or cytosine, especially in the spectral region 3500–3100 cm^{-1} which is for –NH stretching. On the other hand Poly A based nanocapsules showed broad prominent FT-IR peaks at around 3400 cm^{-1} and 3413 cm^{-1} in the presence of thymine and uracil, respectively, which were absent in individual thymine or uracil. Similarly, the peak at around 3200 cm^{-1} for free thymine and 3111 cm^{-1} for free uracil were absent in poly A based nanocapules in the presence of thymine or uracil. This confirms there is a strong base pair interaction between adenine moiety present in Poly A based nanocapsule and that of uracil or thymine, which is as expected and validates our hypothesis on change in fluorescence lifetime. At the same time, it is also true that specific interaction between adenine moiety of Poly A in nanocapasules and thymine/uracil does not impact remarkably fluorescence of the curcumin conjugated Poly A based nanocapsules. However, guanine did not show any specific interaction with Poly A based nanocapsules in the FT-IR spectrum.

To confirm whether adenine moiety present in Poly A had any role in fluorescence amplification in the presence of guanine, we prepared PAH based curcumin conjugated nanocapsules by using PAH instead of Poly A and keeping all other experimental conditions the same. Similar nanocapsules were obtained which had an emission maximum at ~547 nm. The fluorescence intensity, however, increased marginally 20–35% for most of the nucleobases, which is in the line of results obtained for Poly A based nanocapsules, but the fluorescence enhancement was significantly > 265% in the presence of guanine (see Fig. 4A), which is less than observed in the case of Poly A based nanocapsules. These results make us suspect that the interaction between guanine and Poly A nanocapsules is largely due to hydrophobic interaction. This is further supported by the relatively poor solubility of guanine compared to other nucleobases in water.

Realizing the importance of Poly A based nanocapsules for selective sensing of guanine, the calibration curve for estimation of guanine by using Poly A based nanocapsules as fluorescence sensing material was tested. The fluorescence spectra of Poly A based nanocapsules in the presence of different concentrations of guanine did not show any remarkable change in emission maximum. The corresponding fluorescence intensity alteration with guanine concentration is plotted in Fig. 4B. As can be seen in the plot, in a wide range of concentration from 0–7 mM, the curve shows a linear fit. Available methods for guanine estimation work in lower concentration range as given in Table 1. Wang et al. have reported a linear dynamic range of 165–4957 μM for guanine estimation using micellar electrokinetic chromatography with indirect laser-induced fluorescence detection method (Wang et al., 2008). However, the present method showed a wider linear dynamic

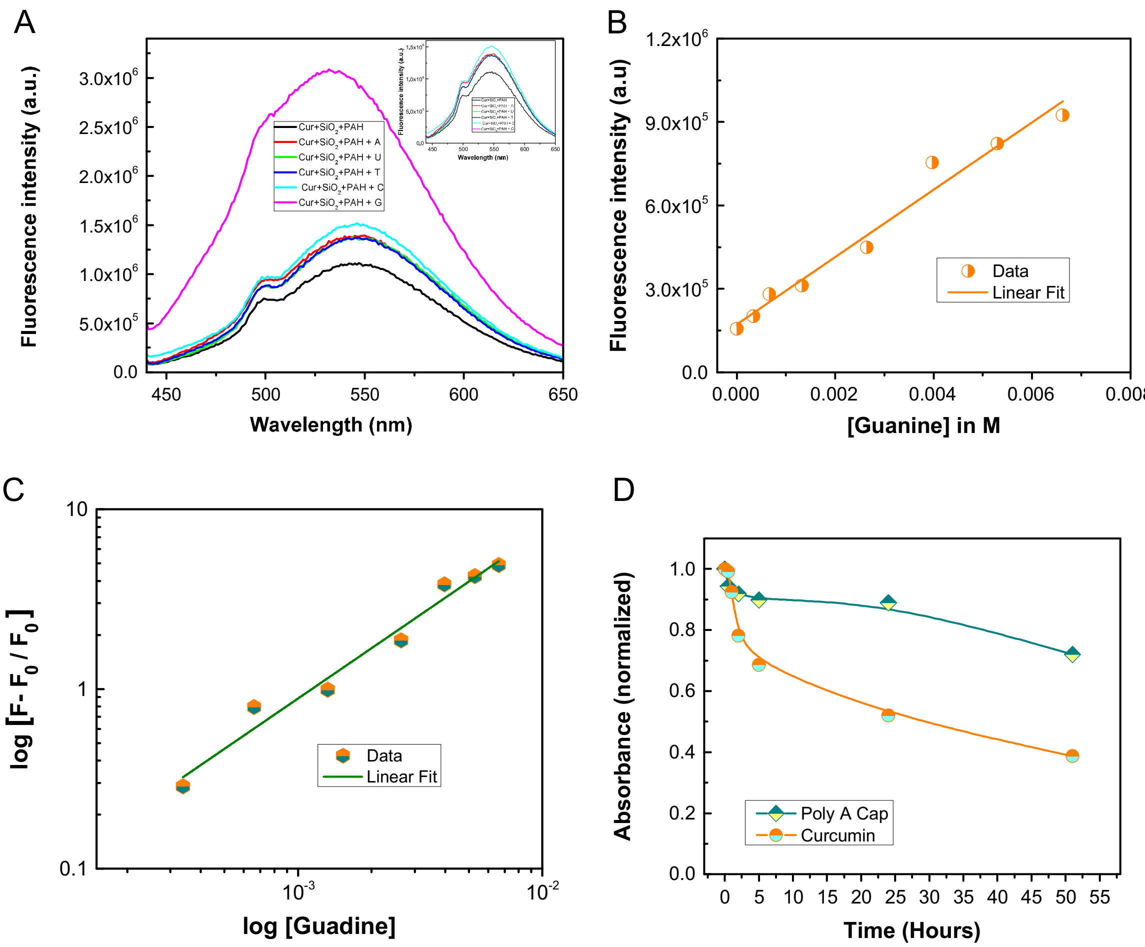

Fig. 4. (A) Fluorescence spectra of aggregates containing silica NPs, curcumin and PAH in the presence of various nucleobases, excited at 425 nm (inset shows rescaled spectra of aggregates without guanine). (B) Linear change in fluorescence intensity of Poly A nanocapsules with guanine concentration. The excitation wavelength was 425 nm and the emission wavelength was 526 nm. (C) Plot of concentration of $(F-F_0)/F_0$ vs. guanine concentration for estimation of binding constant. (D) Stability of Poly A nanocapsules compared to curcumin in buffer solution at pH 7.5. The curcumin solution contained about 8% methanol.

Table 1
Analytical methods for guanine estimation and their linear dynamic ranges.

Method/reagent	Linear dynamic range (μM)	Limit of detection	Reference
Chemiluminescence method using phenylglyoxal	0–100	4 nM	Kai et al. (1994)
HPLC with post-column fluorescence derivatization using phenylglyoxal reagent	1–25	1 μM	Yonekura et al. (1994)
Liquid chromatography with fluorometric detection using 3,4-dimethoxyphenylglyoxal (DMPG)	0–0.4	1 nM	Ohba et al. (1994)
Electrochemical method based on graphene–ionic liquid–chitosan composite film modified glassy carbon electrode	2.5–150	0.75 μM	Niu et al. (2012)
Flow injection chemiluminescence method using hydrogen peroxide	2–600	1.9 μM	Mei et al. (2005)
Electrochemical approach based on electrodeposition of a nanostructured platinum thin film on a glassy carbon electrode	0.1–500	31 nM	Chatterjee and Chen (2012)
Micellar electrokinetic chromatography with indirect laser-induced fluorescence detection	165–4957	2 μM	Wang et al. (2008)
Our method	300–7000	90 μM	

range than the reported one. Nevertheless, the present method is not expected to reach lowest detection limit of the methods applied in low concentration ranges as given in Table 1 due to its applicability in higher concentration ranges.

The association constant of guanine with poly A based nanocapsules is estimated using the following equation (Connors, 1987):

$$\log\left[\frac{(F-F_0)}{F_0}\right] = \log(K) + n\log[\text{guanine}]$$

where K and n are the binding constant and the number of binding sites, respectively. F and F_0 are the fluorescence intensity of Poly A based nanocapsules at excitation wavelength 425 nm and emission wavelength 526 nm in the presence and absence of Poly A nanocapsules, respectively. The association constant of guanine with Poly A based nanocapsules was estimated to be $K=5.50\times10^2\ \text{M}^{-1}$ and the number of binding sites $n=0.93$, which is close to 1 as obtained from the graph in Fig. 4C. Since poly A based nanocapsules are much bigger in size (hundreds of nm) compared to size of guanine (less than nm), the possibility of more than one guanine molecule binding to Poly A based nanocapsule could not be ruled out. It is also important to note that one Poly A based nanocapsule has multiple numbers of curcumin units and the present *n* values might be because of binding between guanine and curcumin.

One of the serious concerns about fluorescence probe, especially for curcumin, has been its stability. Studies have shown that the degradation of curcumin in aqueous solution is linked to hydrolysis that occurs rapidly at a pH above neutrality. HPLC data has proven that curcumin degrades to form *trans*-6-(4′-hydroxy-3′-methoxyphenyl)-2,4-dioxo-5-hexanal as the main product, which further decomposes to vanilin, ferulic acid, and feruloyl methane (Wang et al., 1997). In UV–visible spectral region curcumin exhibited an intense absorption peak around 400–425 nm in neutral aqueous environment. In aqueous solution, there are three pK_a values at 8.38, 9.88 and 10.51 corresponding to deprotonation of the three hydroxyl groups of curcumin (Bernabé-Pineda et al., 2004). It has been established that the contribution of condensation products to the total absorption signal of curcumin are relatively minor, thus, decrease in the visible absorbance over time can be used as a measurement for degradation of curcumin (Leung et al., 2008). Therefore, to understand the stability of the present sensing material, the absorbance change of curcumin and Poly A based nanocapsule was monitored at 427 nm with time in buffer solution as depicted in Fig. 4D. The absorption maximum of curcumin in buffer (7% methanol) at pH 7.5 decayed relatively quickly in the first 5 h (30% degradation) and approximately 62% of the original value in 50 h. On the other hand, the degradation of Poly A based nanocapsules in buffer at pH 7.5 was just 10% in the first 5 h. Further with time the degradation was even slower with 28% degradation after 50 h, which confirmed that degradation of curcumin could be overcome by conjugating with Poly A based nanocapsules for better analytical applicability, which validates robustness of present method.

4. Conclusion

Poly A in the presence of silica nanoparticles formed nanocapsules, which could be conjugated with curcumin. The morphology of these nanocapsules suggests the formation of nanocapsules is due to self-assembly process. In comparison to curcumin–silica NPs complex, curcumin conjugated nanocapsules were much more beneficial to amplify selectivity for estimation of guanine among other nucleobases indicating Poly A plays a significant role in such amplification. However, fluorescence intensity of the nanocapsules was not remarkably influenced by the specific interactions between adenine moiety of Poly A and individual thymine/uracil present in the solution as concluded from FT-IR and fluorescence measurements. The fluorescence intensity of the curcumin conjugated Poly A based nanocapsules was rather highly affected by hydrophobic interaction between guanine and nanocapsules, which made it possible to design a biosensing method for selective estimation of guanine among other nucleobases. This method was applicable to a wider linear dynamic range in higher concentration range compared to the reported methods. The interaction between guanine and nanocapsules was found to be stronger and proposed an association of multiple numbers of curcumin units present in nanocapsules and guanine. The nanocapsules proved to improve degradation of curcumin in aqueous environment. In conclusion, nanotechnology based method in combination of fluorescence probe, nanoparticles, and polymers could be an alternative efficient method for amplifying selectivity and sensitivity of target species as well as improving stability of probe, which builds up further research to test combinations of different nanoparticles such as Ag, Au, etc. along with other probe molecules for biosensing applications.

Acknowledgment

Financial support provided by Lebanese National Council of Scientific Research (NCSR), Lebanon and American University of Beirut, Lebanon through URB as well as Kamal A. Shair Central Research Laboratory (KAS CRSL) facilities to carry out this work is greatly acknowledged.

References

Adams, P., Austin, J.J., Braslavsky, I., et al., 2007. In: Mitchelson, K.R. (Ed.), New High Throughput Technologies for DNA Sequencing and Genomics. Elsevier, Amsterdam, The Netherlands (first ed.).
Abbaspour, A., Noori, A., 2008. Electrochemical studies on the oxidation of guanine and adenine at cyclodextrin modified electrodes. Analyst 133, 1664–1672.
Adhikari, R., Mukeerjee, P., Kee, T.W., Petrich, J.W., 2009. Excited-state intramolecular hydrogen atom transfer and solvation dynamics of the medicinal pigment curcumin. J. Phys. Chem. B 113, 5255.
Adhikary, R., Carlson, P.J., Kee, T.W., Petrich, J.W., 2010. Excited-state intramolecular hydrogen atom transfer of curcumin in surfactant micelles. J. Phys. Chem. B 114, 2997–3004.
Brown, W.H., 1987. Introduction to Organic and Biochemistry, fourth ed. Brooks/Cole Publication, Monterey, p. 418.
Blazej, R.G., Goodwin, W., Heath, S.A., Hillenkamp, F., et al., 2005. In: Nunnally, B.K. (Ed.), Analytical Techniques in DNA Sequencing. CRC Taylor and Francis.
Bouhadir, K.H., Abramian, L., Ezzeddine, A., Usher, K., Vladimiro, N., 2012. Synthesis, cyclcopolymerization and copolymerization of 9-(2-diallylaminoethyl)adenine. Molecules 17, 13290–13306.
Bernabé-Pineda, M., Ramírez-Silva, M.T., Romero-Romo, M., González-Vergara, E., Rojas-Hernández, A., 2004. , Determination of acidity constants of curcumin in aqueous solution and apparent rate constant of its decomposition. Spectroch. Acta A **60**, 1091–1097.
Connors, K.A., 1987. Binding constants, The Measurements of Molecular Complex Stability. Wiley, New York.
Chatterjee, S., Chen, A., 2012. Facile electrochemical approach for the effective detection of guanine. Electrochem. Commun. 20, 29–32.
Didenko, V.V., 2006. Fluorescent Energy Transfer Nucleic Acid Probes: Designs and Protocols. Humana Press, Totowa, NJ.
Khopde, S.M., Priyadarsini, K.I., Palit, D.K., Mukherjee, T., 2000. Effect of solvent on the excited-state photophysical properties of curcumin. Photochem. Photobiol. 72, 625–631.
Kai, M., Ohkura, Y., Yonekura, S., Iwasaki, M., 1994. Chemiluminescence determination of guanine and its nucleosides and nucleotides using phenylglyoxal. Anal. Chim. Acta 287, 75–81.
Li, L., Lu, Y.X., Ding, Y.P., Zhang, F.F., Wang, Y.P., 2012. Facile aqueous synthesis of functionalized CdTe nanoparticles and their application as fluorescence probes for determination of adenine and guanine. Can. J. Chem. 90, 173–179.
Leung, M.H., Colangelo, H., Kee, T.W., 2008. Encapsulation of curcumin in cationic micelles suppresses alkaline hydrolysis. Langmuir 24, 5672–5675.
Mahmodian, L., Mohamadi, M.R., Kaj, N., Tokshi, M., Baba, Y., 2008. In: Landers, J.P. (Ed.), Handbook of Capillary and Microchip Electrophoresis and Associated Microtechniques. CRC Taylor and Francis Group (3rd ed.).
Mauslmani, M., Patra, D., 2014. Revoking excited state intra-molecular hydrogen transfer by size dependent tailored made hierarchically ordered nanocapsules. RSC Adv. 4, 8316–8320.
Mei, Y., Ran, L., Dongyan, H., Yuying, G., 2005. A novel flow-injection chemiluminescence system for the determination of guanine. Luminescence 20, 307–310.
Niu, X., Yang, W., Ren, J., Guo, H., Long, S., Chen, J., Gao, J., 2012. Electrochemical behaviors and simultaneous determination of guanine and adenine based on graphene–ionic liquid–chitosan composite film modified glassy carbon electrode. Electrochim. Acta 80, 346–353.
Ohba, Y., Kai, M., Nohta, H., Ohkura, Y., 1994. Alkoxyphenylglyoxals as fluorogenic reagents selective for guanine and its nucleosides and nucleotides in liquid chromatography. Anal. Chim. Acta 287, 215–221.
Patra, D., Barakat, C., 2011. Synchronous fluorescence spectroscopic study of solvatochromic curcumin dye. Spectroch. Acta A 79, 1034–1041.
Patra, D., El Khoury, E., Ahmadieh, D., Darwish, S., Tafech, R.M., 2012. Effect of curcumin on liposome: Curcumin as a molecular probe for monitoring interaction of ionic liquids with 1,2-dipalmitoyl-sn-glycero-3-phosphocholine liposome. Photochem. Photobiol. 88, 317–327.
Patra, D., Amali, A.J., Rana, R.K., 2009. Preparation and photophysics of HPTS based nanoparticle-assempled microcapsules. J. Mater. Chem. 19, 4017–4021.
Shtykov, S.N., Rusanova, T.Y., 2008. Nanomaterials and nanotechnologies in chemical and biochemical sensors: capabilities and applications. Russ. J. Gen. Chem. 78, 2521–2531.
Sassolas, A., Leca-Bouvier, B.D., Blum, L.J., 2008. DNA biosensors and microarrays. Chem. Rev. 108, 109–139.
Sharma, P., Singh, H., Sharma, S., Singh, H., 2007. Binding of gold nanoclusters with size-expanded DNA bases: a computational study of structural and electronic properties. J. Chem. Theory Comput. 3, 2301–2311.

Wang, L., Zhang, Y., Tian, J., Li, H., Sun, X., 2011. Conjugation polymer nanobelts: a novel fluorescent sensing platform for nucleic acid detection. Nucleic Acids Res. 39, e37.

Wang, W.P., Zhou, L., Wang, S.M., Luo, Z., Hu, Z.D., 2008. Rapid and simple determination of adenine and guanine in DNA extract by micellar electrokinetic chromatography with indirect laser-induced fluorescence detection. Talanta 74, 1050–1055.

Wang, Y.J., Pan, M.H., Cheng, A.L., Lin, L.I., Ho, Y.S., Hsieh, C.Y., Lin, J.K., 1997. Stability of curcumin in buffer solutions and characterization of its degradation products. J. Pharm. Biomed. Anal. 15, 1867–1876.

Xu, X., Chen, S., Li, L., Yu, G., Liu, Y., 2008. Photophysical properties of polyphenylphenyl compounds in aqueous solutions and application of their nanoparticles for nucleobase sensing. J. Mater. Chem. 18, 2555–2561.

Yonekura, S., Iwasaki, M., Kai, M., Ohkura, Y., 1994. Determination of guanine and its nucleosides and nucleotides in human erythrocytes by high-performance liquid chromatography with postcolumn fluorescence derivatization using phenylglyoxal reagent. J. Chromatogr. B: Biomed. Sci. Appl. 654, 19–24.

Zhang, X., Guo, Q., Cui, D., 2009. Recent advances in nanotechnology applied to biosensors. Sensors 9, 1033–1053.

Zhu, Y.G., Liu, J.Y., Chen, K., Shu, G.B., Yang, Y., 2013. Cathodic electrochemiluminescence of eosin Y-peroxydisulfate system and its analytical application for determination of guanine. J. Electroanal. Chem. 689, 46–50.